Chris Mann
Dec 6, 2018

Canada-France-Hawaii Telescope – Semester 2019A Proposal

High resolution spectral follow-up of potential habitable zone super-Earth around an M-dwarf using SPIRou

Abstract:
The recent detection of an exoplanet transit around the M-dwarf 2MASS J19221221+1609510 has prompted our request for spectral follow-up of the system. Initial estimates from the stellar and transit parameters hint at the tantalizing possibility of a super-Earth sized planet in the habitable zone of the host star. These estimates, however, are rough and require spectral observations which will constrain the temperature, size, and mass of the host, as well as measure a radial velocity (RV) curve, look for the Rossiter-McLaughlin effect, and investigate the host's limb darkening. We ultimately will place constraints on the mass, size, and density of the planet. We request 14.75 hours of observing time with SPIRou in the 2019A semester, split between high-cadence sequences during the transit event and sporadic observations near RV peaks to sample the RV curve.

Scientific Justification:

We are requesting time to conduct a spectroscopic follow-up of the transiting exoplanet system 2MASS J19221221+1609510, hereafter called 2MJ1922. It is a 9.7 H-magnitude object located at RA: 19h22m12.21s Dec: +16d09m51.0s. A single transit was observed by TESS (the Transiting Exoplanet Survey Satellite) with a midpoint at 2018-11-10 04:09:11 UTC in one of its 27-day coverage zones. From this data release we measure a transit duration ($\Delta t = 2.2$ hrs) and a fractional drop in flux ($\Delta f / f = 0.0019$). This flux ratio indicates a relative size between the planet and host star of $R_p/R_\star = 0.04358$. 2MASS photometric data tentatively place 2MJ1922 as an early-to-mid-type M-dwarf. Using these observed quantities and adopting a radius and mass ($R = 0.3\ R_\odot$, $M = 0.3\ M_\odot$) typical of such an object (Parsons et al. 2018), we were able to make an estimate of the semi-major axis and in turn, the orbital period. We were fortunate enough to observe a second transit with the Dragonfly optical array, solidifying the estimated period to $P = 19.93933 \pm 0.00007$ days. This corresponds to < 25 minutes transit time uncertainty by the end of semester 2019A.

With these rudimentary estimations of stellar mass, radius, and temperature, as well as orbital semi-major axis, we arrive at the tantalizing possibility of this planet being a super-Earth ($\sim 1.4\ R_\oplus$) orbiting in or near the habitable zone ($T_p \approx 280$K) of 2MJ1922. However, the estimated physical and orbital properties of the planet (with the exception of the period) are heavily dependent on the accurate determination of stellar properties for the host (see Appendix for calculations).

To better characterize the host star as well as the orbital system, we propose a series of spectroscopic observations. Spectra of the host will allow us to characterize spectral features that are tightly linked to metallicity, surface gravity, and temperature (e.g. Mann et al. 2013a, b). This will lead to a more robust estimate of the stellar radius, mass, and temperature. Obtaining spectra during the transit will break the observational degeneracy between the orbital inclination and limb darkening, as both have similar effects on the transit light curve, but only the latter is wavelength dependent. Additionally, if 2MJ1922 happens to be a fast-rotator the Rossiter-McLaughlin effect may be evident and break the $v\sin(i_\star)$ degeneracy between the rotation of the star and its inclination (which may be different than the orbital inclination, i_p).

Of perhaps the most interest, is obtaining radial velocity measurements throughout different phases of the orbit. The orbit is very likely near-circular since our search for a second transit was successful and assumed circular orbit. Based on our rough estimation of the stellar and planet masses, we derive a sinusoidal stellar RV curve with a semi-amplitude of 1.52 m/s (see Fig. 1 and Appendix). Fitting this curve will constrain the true eccentricity of the system and produce a mass

estimate for the planet. This will allow us to assess a bulk density for the planet and glean some information about its composition.

Of more general interest to the astronomical community at large is the addition of a quality set of M-dwarf spectra that span several months. Their ubiquity in the Galaxy (~70% of stars; Lindgren et al. 2016, Covey et al. 2008) and low masses and radii have made M-dwarfs increasingly popular exoplanet search targets. However, their atmospheres are notoriously difficult to model due to poor molecular line lists (Hoeijmakers et al. 2015) and stellar variability (Bell et al. 2012). Building up the pool of high-resolution spectroscopic data sets of M-dwarfs is essential to provide new models with points of comparison. The question of M-dwarf potential habitability is an open one and this system may shed light on possibilities and demographics within these systems.

Technical Justification:

We are requesting to use the SPIRou spectrometer instrument in the Stokes I (intensity) measurement configuration as we are more interested in conserving observation time than investigating magnetic phenomena. We will employ the thermalized Fabry-Pérot etalon in the simultaneous calibration channel for optimal wavelength calibration in order to achieve maximal RV precision. We aim to achieve close to the meter-per-second accuracy indicated by the SPIRou specifications. Figure 1 shows that 24 observations near the RV peaks is sufficient to achieve an amplitude uncertainty near 0.25 m/s.

SPIRou offers very wide wavelength coverage (0.98 – 2.35 μm). This regime contains many of the common metallicity indicators in M-dwarfs (e.g., Ca I and Na I doublet, see Fig. 2) as well as over 500 known absorption lines that can be used for better characterization of the target. For an accurate spectral classification and study of 2MJ1922 itself, we deem it necessary to integrate up to a SNR of ~100. As seen in Figure 3, certain diagnostically useful lines typical of M-dwarfs (Na I and Fe I & II among others) are lost or severely distorted with lower SNR. The SPIRou ETC indicates that an 800s exposure for our 9.7 H-mag target will return a SNR of ~100 using somewhat conservative atmospheric conditions. Our target is comfortably within SPIRou's upper sensitivity limit of H ~ 14.

We divide our observations into two major types. **(1) On-transit observations** have precisely scheduled time requests, and each will consist of 20 exposures of 800s each. The 20 exposures span 4.49 hours (including overheads) and capture the entire transit as well as baseline levels before and after. There are 4 transit events observable from Mauna Kea during semester 2109A. We request coverage for 2 of them, totalling 8.98 hours, as program scheduling and weather permit. **(2) Off-transit observations** do not have a set observing schedule. In order to characterise the RV curve for the rest of the orbit, we request 24 observations at various phases clustered around RV peaks for optimal constraining power (see Fig. 1 inset). Each of these 24 observations will consist of a single 800s exposure, totalling 5.77 hours (including overheads). These 24 exposures can be scheduled flexibly throughout the semester according to weather and observing program density. We request no more than 2 off-transit observations be taken in a single night. The total requested time is thus 14.75 hrs. Tables 1 and 2 list observing specifics and Off-transit observing windows, respectively. Overheads were calculated as 60s per target acquisition and 6s of readout time per exposure.

References:

Allard et al. 2012a, PTRSLSA, 370, 2765
Allard et al. 2012b, EASPS, 57, 3-43
Baraffe et al. 2015, A&A, 577, A42
Bell et al. 2012, PASP, 124.911, 14
Covey et al. 2008, AJ, 136.5, 1778
Hoeijmakers et al. 2015, A&A, 575, A20
Lindgren et al. 2016, A&A, 586, A100
Mann et al. 2013a, AN, 334, 1-2, 18
Mann et al. 2013b, AJ, 145.2, 52
Parsons et al. 2018, MNRAS, 481.1, 1803-1096
Veyette et al. 2016, ApJ, 828.2, 95

Chris Mann
Dec 6, 2018

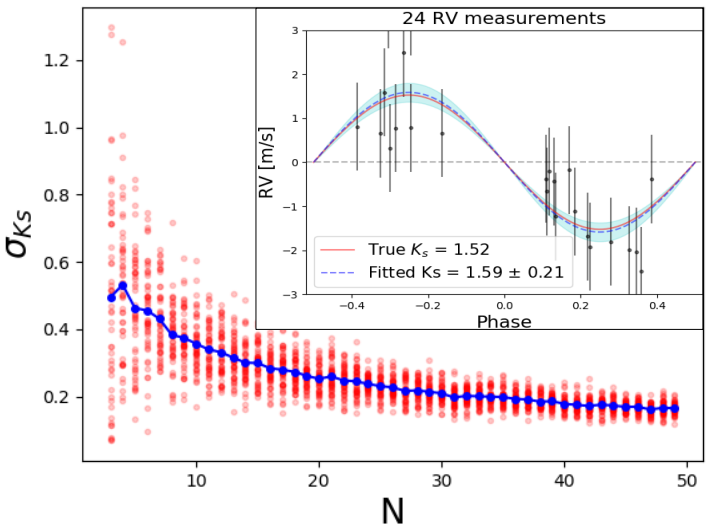

Figure 1: *Inset:* Example of synthetic RV measurements generated from a circular orbit with $M_\star = 0.3\ M_{Sun}$ and $M_p = 2.9\ M_\oplus$ and assuming a measurement uncertainty of 1 m/s. With 24 measurements clustered near the RV peaks, we expect to achieve an amplitude uncertainty near 0.25 m/s. *Background:* Uncertainty in amplitude fit as a function of # of observations. Each N was sampled 50 times. Sensitivity does not significantly improve beyond 24 measurements.

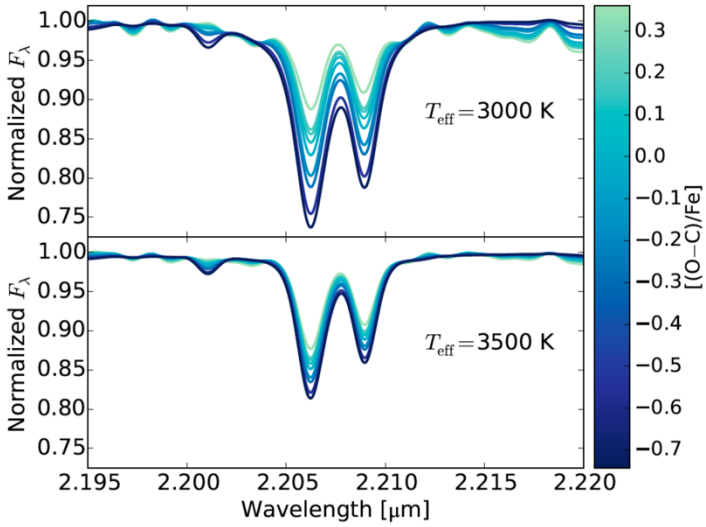

Figure 2: Shown here is the prominent Na I doublet. There are several lines blended with the doublet here, making it very sensitive to the metallicity of the object. This feature can be used as a diagnostic for stellar metallicity. Figure is from Veyette et al. 2016.

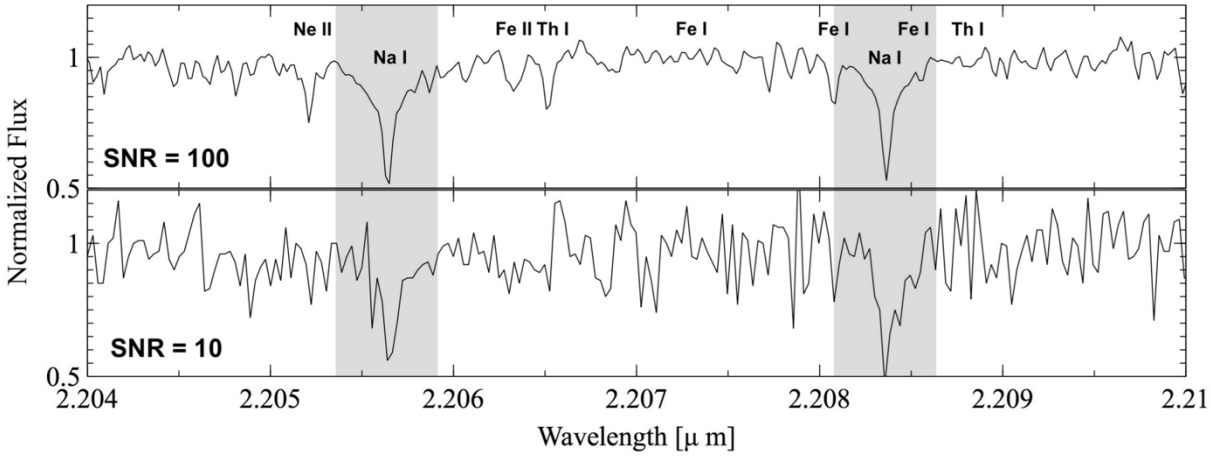

Figure 3: BT-Settl atmospheric model (Allard et al. 2012a, b; Baraffe et al. 2015) of an M-dwarf with parameters: T_{eff} =3100K, log(g) = 4.5 and [Fe/H] = 0.3. Model is shown at SPIRou's native resolution (R~75,000), with SNR modified for each panel. Detailed characterization of spectral features requires high SNR. Note that this is a very small portion of SPIRou's simultaneous 0.98-2.35 μm wavelength coverage.

Chris Mann
Dec 6, 2018

Description	Observation Start (UTC)	# of exp.	Exp. time (s)	Total time with overheads (hrs)
<u>On-Transit</u> Any 2 of these 4 as scheduling permits Subtotal: 8.98 hrs	2019-03-29 10:47:07	20	800	4.49
	2019-04-18 09:19:24	20	800	4.49
	2019-05-08 07:53:57	20	800	4.49
	2019-05-28 06:25:17	20	800	4.49
<u>Off-Transit</u> 24 single exposures of 800s in prescribed observing windows as scheduling permits Subtotal: 5.77 hrs	Variable (see Table 2)	24	800	5.77 (14.4 min each)
Total: 14.75 hrs				

Table 1: Observing plan breakdown. Multiple options are given to improve flexibility of observing program.

Table 2: Observation windows for the Off-transit exposures. The given dates are inclusive. Nights where dusk at Mauna Kea corresponds to the shown UTC date ranges are deemed acceptable.

	Observation Windows (UTC dates)	
	Start	End
24 single exposures of 800s spread throughout these observing windows as scheduling permits. We request no more than 2 observations be taken in a single night.	2019-02-02	2019-02-05
	2019-02-10	2019-02-15
	2019-02-20	2019-02-25
	2019-03-02	2019-03-07
	2019-03-12	2019-03-17
	2019-03-22	2019-03-27
	2019-04-01	2019-04-06
	2019-04-11	2019-04-16
	2019-04-21	2019-04-26
	2019-05-01	2019-05-06
	2019-05-11	2019-05-16
	2019-05-21	2019-05-26
	2019-05-31	2019-06-05
	2019-06-10	2019-06-15
	2019-06-20	2019-06-25
	2019-06-30	2019-07-05
	2019-07-09	2019-07-14
	2019-07-19	2019-07-24
	2019-07-29	2019-07-31

Chris Mann
Dec 6, 2018

Appendix – Supplementary calculations:

If the reviewer is interested in how we estimated preliminary system parameters, see below.

The following relations were calculated using the measured $\Delta t = 2.2$ hrs, and $\Delta f / f = 0.0019$. Values of $R_\star = 0.3\ R_\odot$, $M_\star = 0.3\ M_\odot$, and $T_\star = 3300$ K are assumed as rough stellar estimates.

The radius of the planet can be estimated because the flux decrease during transit is related to the relative areas of the planet and star:

(1) $$\left(\frac{R_p}{R_\star}\right)^2 = \frac{\Delta f}{f} \quad \longrightarrow \quad R_p = R_\star \sqrt{\frac{\Delta f}{f}}$$

The semi-major axis can be estimated by assuming a circular orbit and setting the velocity of the planet crossing the stellar disk as equal to a circular orbital velocity (also assumes impact parameter is close to zero):

(2) $$v_p = \frac{\Delta x}{\Delta t} = \frac{2R_\star}{\Delta t} = \sqrt{\frac{GM_\star}{a}} \quad \longrightarrow \quad a = \left(\frac{\Delta t}{2R_\star}\right)^2 GM_\star$$

The period is easily calculated once we have a semi-major axis by Kepler's 3rd Law:

(3) $$\left(\frac{P}{\text{year}}\right)^2 = \left(\frac{M_\star}{M_\odot}\right)^{-1} \left(\frac{a}{\text{au}}\right)^3$$

The surface temperature of the planet is given by equating stellar insolation and thermal output of the planet. This estimate does not consider albedo, greenhouse, or emissivity effects which could affect drastic change in this quantity:

(4) $$\frac{4\pi R_\star^2 \sigma T_\star^4}{4\pi a^2}(\pi R_p^2) = 4\pi R_p^2 \sigma T_p^4 \quad \longrightarrow \quad T_p = T_\star \sqrt{\left(\frac{R_\star}{2a}\right)}$$

Based on the size of the planet, we assume a density consistent with rocky composition and estimate the planet mass:

(5) $$M_p = \frac{4}{3}\pi R_p^3 \rho_p$$

The amplitude of the RV curve can be calculated from the period, host mass, planet mass, orbital inclination, and eccentricity. Assuming $i \approx 90^o$, $e \approx 0$, $M_\star >> M_p$, and converting units produces a simpler relation:

(6) $$\begin{aligned} K_s &= \left(\frac{2\pi G}{P}\right)^{1/3} \frac{M_p \sin i}{(M_\star + M_p)^{2/3}} \frac{1}{\sqrt{1-e^2}} \\ &= 28.4\ \text{m/s} \left(\frac{P}{\text{year}}\right)^{-1/3} \left(\frac{M_p}{M_{\text{Jup}}}\right) \left(\frac{M_\star}{M_\odot}\right)^{-2/3} \end{aligned}$$

The assumptions made in (6) are reasonable because: simply observing a transit ensures $i \approx 90^o$, our period estimation for finding a second transit was successful while using a circular approximation, and the flux ratio tells us the planet is *much* smaller than the star. Even if the planet mass is large, this will only increase the RV signal.